Sampling of Tissues with Laser Ablation for bottom-up Proteomics: Comparison of Picosecond Infrared Laser (PIRL) and Microsecond Infrared Laser (MIRL)

Andrey Krutilin,[†,⊥] Stephanie Maier,[†,⊥] Raphael Schuster[‡], Sebastian Kruber[†], Marcel Kwiatkowski[§], Wesley D. Robertson[†], Dwayne R. J. Miller[†,‖], and Hartmut Schluter[*,§]

[†]Max Planck Institute for the Structure and Dynamics of Matter, Atomically Resolved Dynamics Department, Center for Free Electron Laser Science, Luruper Chaussee 149, 22761 Hamburg, Germany

[‡]University of Hamburg, Martin-Luther-King-Platz 6, 20146 Hamburg

University of Groningen, Groningen Research Institute of Pharmacy, Pharmacokinetics, Toxicology and Targeting, Antonius Deusinglaan 1, 9713 AV Groningen, Netherlands

[§]University Medical Center Hamburg-Eppendorf, Department of Clinical Chemistry, Martinistraße 52, 20246 Hamburg, Germany

[‖]Departments of Chemistry and Physics, University of Toronto, Toronto, Ontario M5S 3H6, Canada

ABSTRACT: The analysis of proteomes directly from tissues requires the proteins to be released from the cells and their compartments and solubilized, which usually is achieved by mechanical homogenization. It was recently shown, that sampling of tissues with the novel picosecond infrared laser (PIRL) offers higher yields of proteins with respect to the total amount and total number of individual proteins in comparison to mechanical homogenization. Furthermore, proteins obtained from tissues by homogenization with PIRL are significantly less enzymatically degraded, giving improved access to the original composition of proteoforms. The effective cold vaporization of tissue with PIRL is very soft, which is responsible for the phenomenon, that even enzymatic activities of proteins in the tissue aerosol are maintained. In contrast, the energy following irradiation of tissue with microsecond infrared laser (MIRL) pulses is not thermally or acoustically confined to the ablated volume. In this study, PIRL (1 J·cm^{-2}) and MIRL (40-60 J·cm^{-2}) were compared for sampling different tissue types for bottom-up proteomics. We showed that PIRL at low fluence is optimal for soft tissue and desired in scenarios were enzymatic activities of proteins must be maintained as well as were no residual tissue damage is a requirement. MIRL could be well suited for scenarios were enzymatic activities must be suppressed within the intact tissue and thermal and acoustic damage is not a concern.

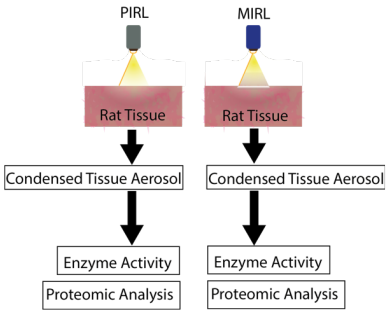

KEYWORDS: laser ablation, tissue sampling & homogenization, proteomics, mass spectrometry

A critical first step in the analysis of proteomes of tissues is the extraction of proteins from their native environment. Depending on the nature of the tissue, different disruption methods are required. Mortar and pestle, Dounce and Potter-Elvehjem grinder, Tissue Lyser, Bead-Mill and Sonification are frequently applied tools for mechanical homogenization of tissues.[1,2,3,4] However, these techniques suffer from requiring relatively large tissue specimens which are needed to generate sufficient amounts of proteins.[5]

One emerging sampling technique is laser capture microdissection (LCM).[6] Here, a tissue specimen is sliced in thin sections and placed into a microscope. A laser then is used to separate the area of interest from the residual tissue for subsequent homogenization and analysis. This procedure preserves spatial information of the selected cells and enables even single cell analysis, but its downsides are the time required for sampling and the problem that fresh frozen tissue is difficult to process. LCM is a two-dimensional approach and an additional homogenization step is required for solubilizing the biomolecules of interest. To overcome these drawbacks it seems reasonable to minimize the time consuming sampling and mechanical homogenization procedure by targeting a laser beam directly onto the tissue area of interest to convert it into an aerosol thereby solubilizing molecules of the tissue, as was recently demonstrated by Kwiatkowski *et al.* and Ren *et al.*[7,8,9] This process reduces the handling of the sample to a single step to minimize losses and changes in sample composition. The novel homogenization technique uses a picosecond infrared laser. Via Desorption by Impulsive Vibrational Excitation (DIVE) the water molecules within the tissue are excited by Picosecond Infrared Laser (PIRL) pulses. In this process, the intramolecular stretching vibrations are induced in the oxygen-hydrogen bonds (O-H) of the water molecules. The vibrational modes are efficiently coupled into translational motions, the very motions involved in driving ablation. This results in an ultrafast transition from liquid to gaseous phase on the timescale of picoseconds driving the tissue into the gas phase faster than any thermal and acoustic energy transfer to the surrounding tissue can occur. [10,11,12] Within the ablation zone a high initial pressure gradient leads to a rapid expansive cooling. Therefore, irradiation with PIRL converts tissue via cold vaporization into an aerosol. Irradiation of tissue with

PIRL induces water molecules of the tissue to act as a propellant completely disrupting the tissue. The condensate of the aerosol after centrifugation shows no pellet demonstrating the high quality of the homogenate.[8] In contrast after mechanical homogenization of tissue, a pellet containing insoluble matter usually remains. Consequently, PIRL sampling of tissue yields a higher number of identified proteins compared to mechanical homogenization.[8] Since the ablation process is very soft, even enzymatic activities in the condensate of PIRL aerosols are preserved.[7] In this study, we compared the qualitative and quantitative yield of proteins in the condensates of two different tissues aerosols of a conventional Er:YAG laser (MIRL) and the PIRL.

MATERIALS AND METHODS

Chemicals, Solvents, and Reagents. All chemicals were purchased from Sigma-Aldrich (Steinheim, Germany) or Fisher Scientific (Bremen, Germany) and used without further purification. Sequence-grade trypsin was purchased from Promega (Mannheim, Germany). Coomassie Brilliant Blue G 250 was purchased from Carl Roth (Karlsruhe, Germany). Unstained Precision protein standards broad range was purchased from Bio-Rad (Munich, Germany).

Sample Preparation. Rat tissue samples from Wister rats were received from the research animal facilities of the Medical Center Hamburg-Eppendorf (UKE). The experiments were performed following the principles of the 3Rs, namely reduction, only tissue of rats that had been sacrificed for other projects. Fresh muscle, liver and kidney tissues were cut in four pieces, immediately frozen in liquid nitrogen and stored prior to ablation at - 80 °C.

Tissue Homogenization. Figure S-1 of the supporting information shows an illustration of the experimental setup. As laser system a PIRL-HP3-1064 OPA-3000 (Attodyne Inc., Toronto, Canada) and a commercial MIRL (Er:YAG laser, MEY-1-A EX-2, J Morita Mfg Corp., Kyoto, Japan) was used for the experiments. Both lasers emitted a Gaussian shape beam with a wavelength of 3000 ± 90 nm for PIRL and 2.94 μm for MIRL. The pulse duration of the PIRL and MIRL were 400 ps and 300 μs, respectively. Additional laser parameters are described in the supplementary information (Table S-2). These lasers were connected to a home-build scanning system with an autofocus function. The ablation area was adjusted to 4 x 4 mm and the ablation time for each specimen was 260 seconds. The ablated volume depends not only on the applied fluence, but also on the tissue type. It can be estimated that the ablated volume in case of PIRL is around 13 mm^3 in liver tissue. For MIRL the ablated volume in soft tissue can be evaluated to range from around 10 to 20 mm^3 depending on the fluence.[13] A home-build sample stage was used and adjusted to -10 °C. During the ablation process the generated plume was transferred to a cryo-trap via low pressure created by the membrane pump (MZ 2C VARIO, VACUUBRAND GmbH & CO KG, Wertheim, Germany).

Kidney homogenates were used without further preparation for the MALDI analysis (see paragraph below). Muscle and liver homogenates were prepared as followed. After thawing, the samples were quickly aliquoted into two parts. One part was mixed 1:1 (v:v) with 6 M Urea and centrifuged at 15,000 × g for 3 minutes. The supernatants were transferred into a 2 mL reaction vial and stored in 4 °C until the proteomic experiment. The second part was mixed with 100 µL 5x Laemmli buffer (225 mM Tris-HCl, pH 6.8, 50 % glycerol, 5 % sodium dodecyl sulfate; 0.05 % bromophenol blue; 250 mM dithiothreitol,) and immediately transferred in a boiling water bath for 5 minutes. The homogenates were centrifuged at 15,000 × g for 3 minutes. The supernatants were transferred into a 2 mL reaction vial and stored in -20 °C. The protein amounts obtained were measured with a 2-D Quant Kit following the manufactures protocol.

SDS-PAGE. For SDS-PAGE, 30 µg homogenate was loaded on a 10% Bis-Tris gel (Criterion™ XT Bis-Tris gel, Bio-Rad, Munich, Germany). Electrophoresis was performed at a constant voltage of 120 V for 60 minutes. The gel was stained (40% MeOH, 10% acetic acid, 0.025 % Coomassie Brilliant Blue G 250, dissolved in ultrapure water) overnight and distained with 40 % MeOH.

Mass Spectrometry. Tryptic in-solution digestion of tissue homogenates was performed in accordance with Wiśniewski *et al.*[14]and the experiment was carried out in centrifuge filter with a 10 kDa Cut-off. LC-MS/MS analysis was performed using reversed-phase ultra high-performance liquid chromatography (Dionex UltiMate 3000 RSLCnano, Thermo Scientific, Bremen, Germany) coupled via electrospray ionization (ESI) to a quadrupole orbitrap mass spectrometer (Orbitrap Fusion, Thermo Scientific, Bremen, Germany). For the LC-MS/MS analysis, 5 µL of the original homogenates from MIRL and PIRL were used for the acquisition of LC-MS/MS data (Xcalibur Software Version 3.1). The samples were loaded on a trapping column (nanoACQUITY UPLC Symmetry C18 trap column, 180 µm × 20 mm, 5 µm, 100 Å; buffer A: 0.1 % formic acid in ultra-pure water; buffer B: 0.1 % formic acid in acetonitrile, Waters, Manchester, U.K.) at a flow rate of 5 $nl \cdot min^{-1}$ with a 2 % buffer B for 5 minutes. In the next step, the analytes were transported into the separation column (nanoACQUITY UPLC column, BEH 130 C18, 75 µm × 250 mm, 1.7 µm, 100 Å, Waters, Manchester, U.K.) and passed through with a flow rate of 200 $nL \cdot min^{-1}$. A 60 minutes separation gradient from 2-50 % B was used to elute the proteins. For spray generation a fused-silica emitter (I.D. 10 µm, New Objective, Woburn, USA) at a capillary voltage of 1650 V was used. For data acquisition, the mass spectrometer was performed in positive ion mode.

Data Processing. Proteins were identified from the LC-MS/MS raw data with the MaxQuant Software (Version 1.5.2.8, Max Planck Society, Munich, Germany) using the Andromeda search engine against the *rattus norvegicus* Uniprot-Swiss-Prot database (www.uniprot.org, downloaded January 29, 2016, 7934 sequence entries). The search parameters were defined to allow a precursor tolerance of 10 ppm and MS/MS tolerance of 0.6 Da, variable modifications of methionine oxidation as well as carbamidomethylation for cysteine residues, and two missed cleavages were allowed. Only proteins identified with at least two unique peptides were taken into account.

MALDI analysis. The MALDI analysis was used to determine the enzyme activities by measuring the degradation products of angiotensin I (Ang 1-10). Prior to MALDI analysis the homogenates were incubated in angiotensin I ($c_{Ang1\text{-}10} = 10^{-5}$ M, 1:9, v:v, homogenate: Ang 1-10) for 0, 3, 6 and 24 hours. For each time point the mixture was mixed with DHB (2,5-Dihydroxybenzoic acid 20 $mg \cdot ml^{-1}$ in 50% ACN, 0,1% TFA) in a volume ratio of 1:2 (v:v), respectively. The samples were stored at 4 °C for further measurement. The

MALDI spectra were recorded via a time-of-flight (TOF) mass spectrometer (Bruker UltrafleXtreme Smartbeam II Laser, Bremen, Germany) and each spectrum was generated through 2000 shots in partial sample mode. The instrument was operated in positive reflector ion mode, a repetition rate of 20 Hz, 40 % laser intensity, 20 kV first acceleration voltage, 18.5 kV second acceleration voltage and 250 ns extraction delay. The recorded m/z range was from 500-5040.

RESULTS AND DISCUSSION

Total protein amounts in the condensates of the tissue aerosols. Rat liver (n = 9) and muscle (n = 9) tissue was ablated with each laser system and the total amount of protein contained within the collected condensate measured. For rat liver tissue, 470 ± 188 µg and 216 ± 131 µg of protein was measure for ablation by PIRL or MIRL, respectively, in the condensates (Table S-3). The condensates of rat muscle tissue obtained with PIRL and MIRL yielded 342 ± 142 µg and 479 ± 208 of proteins, respectively.

Surface of ablated area. Figure 1 shows the ablated areas of kidney tissue after the exposure time of 260 seconds with PIRL and MIRL. The ablated volume can be seen as a rectangular pattern. The remaining tissue after ablation with PIRL exhibited no visible changes and has a planar surface. In contrast, the MIRL ablated tissue shows burnt residue around the irradiation area. The ablation surface is formed by laser pulse impact. The post-ablation results of the surface for muscle and liver tissue are shown in the supplementary section Figure S-4 and Figure S-5.

SDS-PAGE for Muscle and Liver Tissue. In figure 2, two technical replicates are presented for liver (A) and muscle (B) homogenate using PIRL with 1 J·cm^{-2} and MIRL with 40 and 60 J·cm^{-2}, respectively. A general comparison of the lanes from PIRL (L1, L2) and MIRL (L3, L4) in the condensates of the aerosols of liver (A) showed a similar pattern, however different distribution of the ratio of intensities of the protein bands was observed.

The protein patterns in the condensates of the aerosols of rat muscle tissue (B) obtained by PIRL (M1, M2) and MIRL (M3, M4) are similar, as well. Nearly all protein bands are present in both cases, however again there are significant differences in the ratio of the intensities of the bands which appear to be protein weight dependent. In the region of 3 kDa to 6 kDa of all SDS-PAGE gels of condensates of the tissue aerosols obtained with MIRL a gradient band is shown.

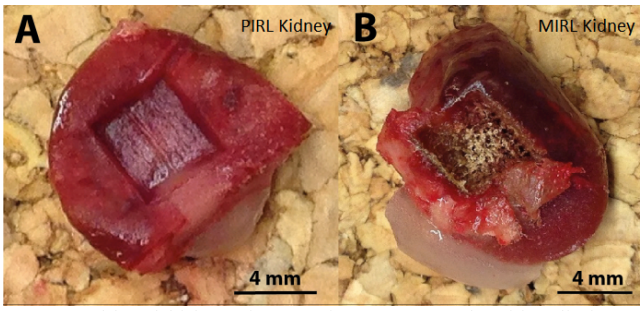

Figure 1. Ablated kidney tissues after 260 seconds of irradiation with PIRL (A) and MIRL (B). The 4 x 4 mm areas were ablated in both cases. Burnt residue is observed after MIRL irradiation. The adjacent tissue after PIRL irradiation indicates no significant alteration to the naked eye and appears red and moist.

This band is not present in the SDS-PAGE gels of the condensates of the tissue aerosols obtained with PIRL. Since the increased intensity of the 3 kDa to 6 kDa band in the samples obtained with MIRL might have been formed by staining of fragments from proteins being much larger than 3 kDa to 6 kDa, these bands were cut and subjected to tryptic digestion, followed by LC-MS/MS analysis, but the results showed a similar number of proteins for both lasers in this region (data not shown). Thus it can be excluded that the increased staining of the 3 kDa to 6 kDa band was due to the binding of Coomassie to either a higher number of small proteins or protein fragments.

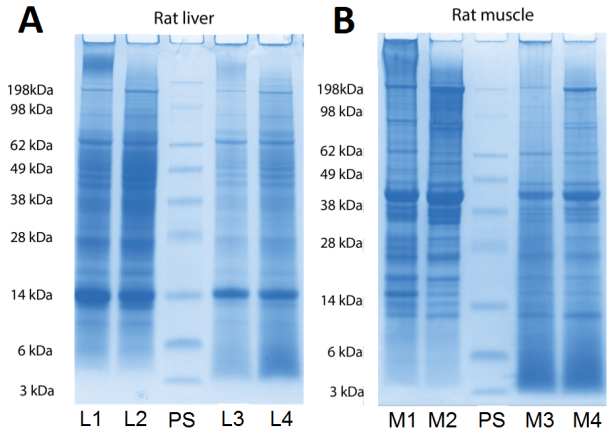

Figure 2. SDS-PAGE of the homogenates of the tissue aerosols produced by irradiation of **liver (A)** and **muscle (B)** with PIRL and MIRL. The PIRL samples (L1, L2, M1 and M2) were obtained with an average fluence of 1 J·cm^{-2}. Ablation with MIRL was performed with 40 J·cm^{-2} (samples L3 and M3) and 60 J·cm^{-2} (samples L4 and M4). PS: protein standard.

Statistical analysis of the LC–MS/MS data of the condensates of the PIRL and MIRL induced aerosols of muscle and liver tissue. The efficiency of the extraction of the proteins from tissue induced by laser ablation, for both the PIRL and MIRL was investigated by subjecting the condensates of the aerosols of muscle and subjected to statistical analysis of the LC–MS/MS data. Figure 3 summarizes the results.

A higher number of proteins were identified with MIRL ablation on the rat muscle tissue. Due to the higher fluences in the case of MIRL, the ablation depth per pulse is considerable higher on the order of several tens of micrometers compared to PIRL.[15] Therefore, a precise layer-by layer ablation with an ablation depth per laser pulse of a few micrometers as in case of PIRL was not achieved in this experiment. The difference in pulse energy requirements is due to the differences in efficiencies for ablation in the two different pulse regimes. More energy is lost by acoustic transport and thermal diffusion for MIRL relative to PIRL as evident in Figure 1 by the burning for similar ablation rates with respect to material removal.

The total number of proteins identified from liver by bottom up proteomics following MIRL extraction was 581 proteins and with PIRL 926. From that 326 were identified in both MIRL and PIRL. In contrast, the total number of identified proteins in muscle with MIRL was 883 proteins and with PIRL 642. From that 406 were identified in both MIRL and PIRL.

There is a correlation between the toughness of the tissues and the yield of proteins, both the total amount and the number of individual proteins. It can be assumed that the significant

higher fluence of MIRL in the range of 40 to 60 J cm^{-2} in comparison with PIRL at 1 J·cm^{-2} is responsible for a more effective extraction of the muscle tissue, which is much more robust because of its larger content of connective tissue compared to liver tissue and the actin and myosin filaments within the myocytes. Further studies utilizing higher fluence PIRL should be performed to investigate the effect. The present system is limited in pulse energy for the needed focusing conditions to compare the two pulse regime. In comparison to muscle tissue, liver tissue is much softer and the collagen content is low compared to other tissues.[16] As a result, the fluence used here with the PIRL is high enough for an efficient ablation and homogenization the liver tissue. In consequence, a significant higher yield of the total protein amount and of the number of individual proteins was achieved by the ablation of liver tissue with PIRL in comparison to MIRL.

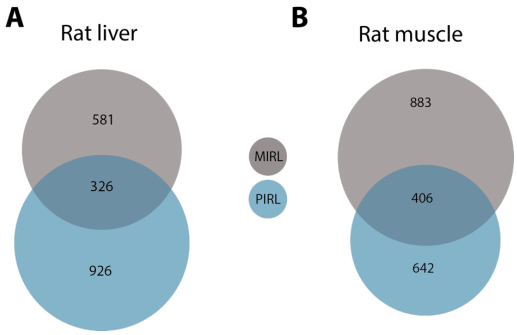

Figure 3. VENN diagram of extracted proteins from rat liver (A) and rat muscle (B) with MIRL and PIRL in a LC-MS/MS analysis. Proteins were counted if 2 or more of their unique peptides have been identified and are detected in two technical replicates of rat liver and muscle, respectively.

Enzyme Activity. The enzymatic activity retained in the condensates of tissue aerosols obtained with MIRL and PIRL was investigated using angiotensin I (amino acid sequence: DRVYIHPFHL), because in renal tissue [17] and in blood [18], which is still present in the tissue, several proteases are present, which can convert angiotensin I into smaller peptides. MALDI-TOF spectra of the reaction products of the incubation of angiotensin I with condensates (see protein concentration measurement Figure S-6) of the aerosols of renal tissue after defined incubation times are shown in Figure 4.

After an incubation time of 3 hours an intense signal of m/z 1181.7 was present, which corresponds to angiotensin 1-9 (DRVYIHPFH) and likely to have been produced by a carboxy-peptidase like the angiotensin-converting-enzyme-2. In addition, signals with smaller intensities are visible with m/z 1046.5 and m/z 899.5, corresponding to angiontensin II (angiotensin 1-8, DRVYIHPF) and angiotensin 1-7 (m/z 899.5, DRVYIHP). These signals indicate enzyme activities of several peptidases like the angiotensin-converting enzymes (ACE1 and ACE2), chymase and/or neprilysin.[18] The increase of the signal intensities of the enzymatic degradation products of angiotensin I represents the increasing enzymatic conversion. This feature is beneficial in future to study the enzyme kinetics and reaction directly out of a tissue sample.

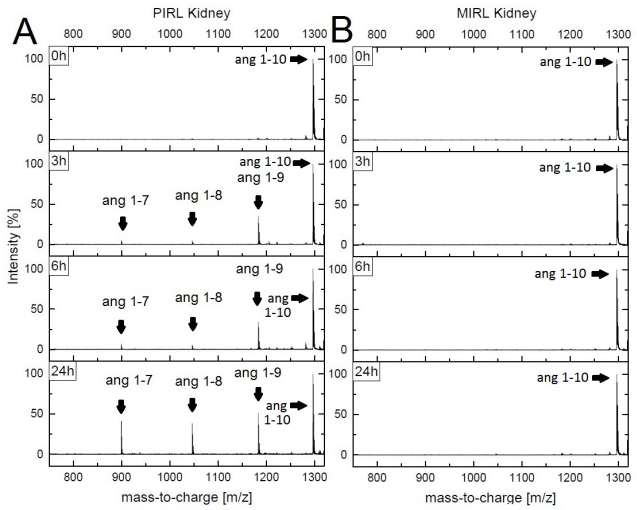

Figure 4. MALDI-TOF mass spectra of angiotensin 1-10 (c = 10^{-5} M) incubated with the condensates of the aerosols obtained from renal tissue by (A) PIRL (B) MIRL. The reaction mixtures were analyzed after 0 h, 3 h, 6 h, and 24 h incubation time. Signals of the generated angiotensin peptides and angiotensin 1-10 are marked by arrows. Matrix: 2,5-Dihydroxybenzoic acid (2,5-DHB).

In contrast, the MALDI spectra of the incubation of angiotensin I with the condensate of the aerosol of renal tissue, obtained with MIRL, showed no signals even after an incubation time of 24 h, indicating that no significant enzymatic activities were present. It can be assumed that this result is related to the heating of the adjacent tissue, which occurs during irradiation of tissue with MIRL as well as degradation of the species during ablation. The heating effect of MIRL is already very obvious on the surface of the ablation zone (Fig.1) and is likely responsible for the denaturing proteins and thereby inactivating enzymes.

CONCLUSION

In this study, we utilized a commercial microsecond infrared laser (MIRL), which is typically used in surgery, for ablation of liver and muscle tissue and compared the results with respect to the total protein amount, number of identified individual proteins and enzymatic activities with the new picosecond infrared laser (PIRL). PIRL extraction produced more identifiable proteins from soft tissue, rat liver, at a considerable lower fluence (1 J·cm^{-2}). However, for rat muscle tissue containing a higher content of connective tissue MIRL at high fluence (40 to 60 J·cm^{-2}) resulted in more identified proteins than PIRL. In contrast to MIRL, PIRL did not induce residual tissue burning or damage and maintained enzymatic activities of the extracted species. Thus, PIRL is the first choice for tissue sampling in which minimal disruption to the species of interest as well as the sample tissue itself is desired. The application of MIRL could be suited for scenarios with tough tissue types were thermal and acoustic damage is not a concern and / or if enzymatic activities must be suppressed within the intact tissue already. The results suggest increasing penetration depth of PIRL ablation with increased pulse energies could be an optimal solution for sampling rigid tissue.

ASSOCIATED CONTENT

Supporting Information. Additional information as noted in text. This material is available free of charge via the Internet at http://pubs.acs.org.

AUTHOR INFORMATION

Corresponding Author

* Tel.: +49 (0) 40 7410 – 58795; fax: +49 (0) 40 7410 – 54971; e-mail: hschluet@uke.de

Author Contributions

⊥S. M. and A.K. equally contributed to this manuscript.

Notes

Dwayne R. J. Miller is the co-founder of AttoDyne Inc.The authors declare no competing financial interest.

ACKNOWLEDGMENT

We thank the SUREPIRL project (ERC advanced grant, project reference: 291630) for financial support, the research animal facilities of the Medical Center Hamburg-Eppendorf (UKE) for sample support and Djordje Gitaric, Khashayar Shojaei-Asanjan for the design of the ablation box.

ABBREVIATIONS

LCM, Laser capture microdissection; MALDI TOF, Matrix-assisted laser desorption/ionization time-of-flight; SDS PAGE, Sodium dodecyl sulfate polyacrylamide gel electrophoresis; LC-MS/MS, Liquid chromatography tandem-mass spectrometry; MIRL, Microsecond infrared laser; PIRL, picosecond infrared laser; TFA, Trifluoroacetic acid; ACN, Acetonitrile; ESI, Electrospray ionization.

REFERENCES

(1) Aldridge, W. N.; Emery, R. C.; Street, B. W. A Tissue Homogenizer. *Biochem. J.* **1960**, *77* (2), 326–327.

(2) Trimpin, S.; Weidner, S. M.; Falkenhagen, J.; McEwen, C. N. Fractionation and Solvent-Free MALDI-MS Analysis of Polymers Using Liquid Adsorption Chromatography at Critical Conditions in Combination with a Multisample on-Target Homogenization/transfer Sample Preparation Method. *Anal. Chem.* **2007**, *79* (19), 7565–7570.

(3) Geier, F. M.; Want, E. J.; Leroi, A. M.; Bundy, J. G. Cross-Platform Comparison of Caenorhabditis Elegans Tissue Extraction Strategies for Comprehensive Metabolome Coverage. *Anal. Chem.* **2011**, *83* (10), 3730–3736.

(4) Haque, S.; Khan, S.; Wahid, M.; Mandal, R. K.; Tiwari, D.; Dar, S. A.; Paul, D.; Areeshi, M. Y.; Jawed, A. Modeling and Optimization of a Continuous Bead Milling Process for Bacterial Cell Lysis Using Response Surface Methodology. *RSC Adv.* **2016**, *6* (20), 16348–16357.

(5) Shao, S.; Guo, T.; Gross, V.; Lazarev, A.; Koh, C. C.; Gillessen, S.; Joerger, M.; Jochum, W.; Aebersold, R. Reproducible Tissue Homogenization and Protein Extraction for Quantitative Proteomics Using Micropestle-Assisted Pressure-Cycling Technology. *J. Proteome Res.* **2016**, *15* (6), 1821–1829.

(6) Longuespée, R.; Fléron, M.; Pottier, C.; Quesada-Calvo, F.; Meuwis, M.-A.; Baiwir, D.; Smargiasso, N.; Mazzucchelli, G.; De Pauw-Gillet, M.-C.; Delvenne, P.; et al. Tissue Proteomics for the Next Decade? Towards a Molecular Dimension in Histology. *Omi. A J. Integr. Biol.* **2014**, *18* (9), 539–552.

(7) Kwiatkowski, M.; Wurlitzer, M.; Omidi, M.; Ren, L.; Kruber, S.; Nimer, R.; Robertson, W. D.; Horst, A.; Miller, R. J. D.; Schlüter, H. Ultrafast Extraction of Proteins from Tissues Using Desorption by Impulsive Vibrational Excitation. *Angew. Chemie - Int. Ed.* **2015**, *54* (1), 285–288.

(8) Kwiatkowski, M.; Wurlitzer, M.; Krutilin, A.; Kiani, P.; Nimer, R.; Omidi, M.; Mannaa, A.; Bussmann, T.; Bartkowiak, K.; Kruber, S.; et al. Homogenization of Tissues via Picosecond-Infrared Laser (PIRL) Ablation: Giving a Closer View on the in-Vivo Composition of Protein Species as Compared to Mechanical Homogenization. *J. Proteomics* **2016**, *134*, 193–202.

(9) Ren, L.; Robertson, W. D.; Reimer, R.; Heinze, C.; Schneider, C.; Eggert, D.; Truschow, P.; Hansen, N.-O.; Kroetz, P.; Zou, J.; et al. Towards Instantaneous Cellular Level Bio Diagnosis: Laser Extraction and Imaging of Biological Entities with Conserved Integrity and Activity. *Nanotechnology* **2015**, *26* (28), 284001.

(10) Vogel, A.; Venugopalan, V. Mechanisms of Pulsed Laser Ablation of Biological Tissues. *Chem. Rev.* **2003**, *103* (2), 577–644.

(11) Franjic, K.; Miller, D. Vibrationally Excited Ultrafast Thermodynamic Phase Transitions at the Water/air Interface. *Phys. Chem. Chem. Phys.* **2010**, *12* (20), 5225–5239.

(12) Franjic, K.; Cowan, M. L.; Kraemer, D.; Miller, R. J. D. Laser Selective Cutting of Biological Tissues by Impulsive Heat Deposition through Ultrafast Vibrational Excitations. *Opt. Express* **2009**, *17* (25), 22937–22959.

(13) Walsh, J. T.; Deutsch, T. F. Er:YAG Laser Ablation of Tissue: Measurement of Ablation Rates. *Lasers Surg. Med.* **1989**, *9* (4), 327–337.

(14) Wiśniewski, J. R.; Zougman, A.; Nagaraj, N.; Mann, M. Universal Sample Preparation Method for Proteome Analysis. *Nat. Methods* **2009**, *6* (5), 359–362.

(15) Cummings, J. P.; Walsh, J. T. Erbium Laser Ablation: The Effect of Dynamic Optical Properties. *Appl. Phys. Lett.* **1993**, *62* (16), 1988–1990.

(16) Neuman, R. E.; Logan, M. A. The Determination of Collagen and Elastin in Tissues. *J. Biol. Chem.* **1950**, *186* (2), 549–556.

(17) Rykl, J.; Thiemann, J.; Kurzawski, S.; Pohl, T.; Gobom, J.; Zidek, W.; Schlüter, H. Renal Cathepsin G and Angiotensin II Generation. *J. Hypertens.* **2006**, *24* (9), 1797–1807.

(18) Hildebrand, D.; Merkel, P.; Eggers, L. F.; Schl??ter, H. Proteolytic Processing of Angiotensin-I in Human Blood Plasma. *PLoS One* **2013**, *8* (5).

(19) Loesel, F. H.; Brockhaus, P.; Fischer, J. P.; Götz, M. H.; Noack, F.; Bille, J. F. Comparison of Tissue Ablation by Ultrashort Laser Pulses in the Nano-, Pico- and Femtosecond Range. *Proc. SPIE* **1994**, *2323*, 227–233.

Supporting Information:

Sampling of Tissues with Laser Ablation for bottom-up Proteomics: Comparison of Picosecond Infrared Laser (PIRL) and Microsecond Infrared Laser (MIRL)

Andrey Krutilin,[†,⊥] Stephanie Maier,[†,⊥] Raphael Schuster,[‡] Sebastian Kruber[†], Marcel Kwiatkowski[§], Wesley D. Robertson[†], Dwayne R. J. Miller[†,∥], and Hartmut Schlueter[*,§]

[†]Max Planck Institute for the Structure and Dynamics of Matter, Atomically Resolved Dynamics Department, Center for Free Electron Laser Science, Luruper Chaussee 149, 22761 Hamburg, Germany

[‡]University of Hamburg, Martin-Luther-King-Platz 6, 20146 Hamburg

[§]University Medical Center Hamburg-Eppendorf, Department of Clinical Chemistry, Martinistraße 52, 20246 Hamburg, Germany

[∥]Departments of Chemistry and Physics, University of Toronto, Toronto, Ontario M5S 3H6, Canada

Corresponding Author

* Tel.: +49 (0) 40 7410 – 58795; fax: +49 (0) 40 7410 – 54971; e-mail: hschluet@uke.de

Contents:

1. Schematic setup up of the PIRL and MIRL beam and the equipment for tissue collection during the ablation process

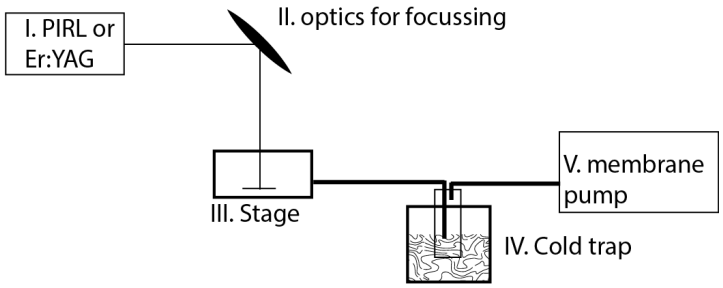

Figure S-1. Schematic setup up of the MIRL (Er:YAG) and MIRL beam and the equipment for tissue collection during the ablation process. I. PIRL or MIRL, II. Optical lenses for focusing III. Stage, IV. Cooling-trap, V. Membrane pump

2. Laser settings and beam characteristics on the sample surface during ablation experiments

The beam spot sizes in the focus of both lasers were measured by a Silicon microbolometer Beam Imaging Camera (WinCamD-FIR-2-16HR, DataRay Inc., Redding, USA). Since the Er:YAG laser and the PIRL have different pulse durations, the threshold of the fluence needed for initiating the ablation process is for PIRL lower than for lasers with longer pulse durations like the Er:YAG laser[19]. Moreover, the Er:YAG laser has a considerable smaller repetition rate than PIRL. To collect enough sample material in a short time period for the subsequent mass spectrometry analysis in case of the Er:YAG laser, a higher fluence was chosen for the experiments. For that reason, the laser pulses for ablation were adjusted to achieve an average fluence of 1 J·cm^{-2}for PIRL and 40 J·cm^{-2}and 60 J·cm^{-2} for the Er:YAG laser on the sample stage. It is expected, that the higher fluences for the Er:YAG laser compared to the PIRL have no crucial influence on the experiment, since the peak irradiance per pulse, for PIRL is with 2.53 GW/cm^{-2} still orders of magnitude higher than for the Er:YAG laser with 0.19-0.38 MW/ cm^{-2}. However, the particle size in the ablation plume correlates with the penetration depth of applied laser pulses [10,11] Thus, a higher fluence as in case of Er:YAG leads to a higher penetration depths and bigger particles in the ablation plume. The low fluence of the PIRL ablation results in a high quality of the homogenate with no pellet formation after centrifugation of the condensate of the ablation plume.[8]

The energy measurement of the laser pulses was conducted with a precision energy meter (LabMax-Top with Energymax Sensor J-25-MB-LE and J-25-MB-HE, Coherent, Santa Clara, USA) and the energy was measured before each ablation of a sample for 60,000 pulses (PIRL) and 1200 pulses (Er:YAG laser). Tab S-2 shows an overview over all laser settings and beam characteristics.

Parameters	PIRL	Er:YAG laser
Wavelength	3 µm	2.94 µm
Pulse width	400 ps	300 µs
Repetition rate	1000 Hz	25 Hz
Beam Diameter (1/e^2)	~ 170 µm	~ 250 µm
Pulse energies (E_p)	230 µJ	28-56 mJ
Average pulse fluence (φ_a)	1 J·cm^{-2}	40-60 J·cm^{-2}
Peak pulse fluence (φ_p)	2 J·cm^{-2}	80-120 J·cm^{-2}
Peak power (P_p)	0.575 MW	93-187 W
Peak irradiance (I_p)	2.53 GW/ cm^{-2}	0.19-0.38 MW/cm^{-2}

Table S-2 Laser settings and beam characteristics on the sample surface during ablation experiments for PIRL and Er:YAG laser.

3. Mean values for protein yields for samples evolved with MIRL and PIRL after irradiation on rat liver and muscle.

	PIRL liver (μg)		PIRL muscle (μg)
Mean	470	Mean	342
STD	188	STD	142
	MIRL liver (μg)		MIRL muscle (μg)
Mean	216	Mean	479
STD	131	STD	208

Table S-3. Mean values for protein yields for samples evolved with MIRL and PIRL after 260 sec. irradiation period on rat **liver and muscle**. The ablation area was adjusted to 4 mm x 4 mm. The mean values arise from the nine homogenates of MIRL and PIRL of rat liver and muscle, respectively.

4.Tryptic digestion of tissue homogenates.

Briefly, reduction and alkylation was carried out with 10 mM dithiothreitol solution and 55 mM iodoacetamide solution in the dark, respectively. Amoniumbicarbonate solution (400 µL, c = 100 mM) and tryptic solution (3 µL, c = 0.25 µg μL^{-1}) were added to the protein samples and stored overnight at 37 °C. After 16 h the digestion was stopped by centrifugation of the samples for ten minutes at 14000 x g. Afterwards the samples were evaporated and dissolved in 100 µL 1% FA for further desalting procedure using Sep-Pak 100 column (Waters, Manchester, UK). After desalting the sample was evaporated and dissolved in 20 µL 0.1% FA for further LC-MS/MS analysis.

5. Ablated rat muscle tissues after ablation with PIRL (A) and MIRL (B).

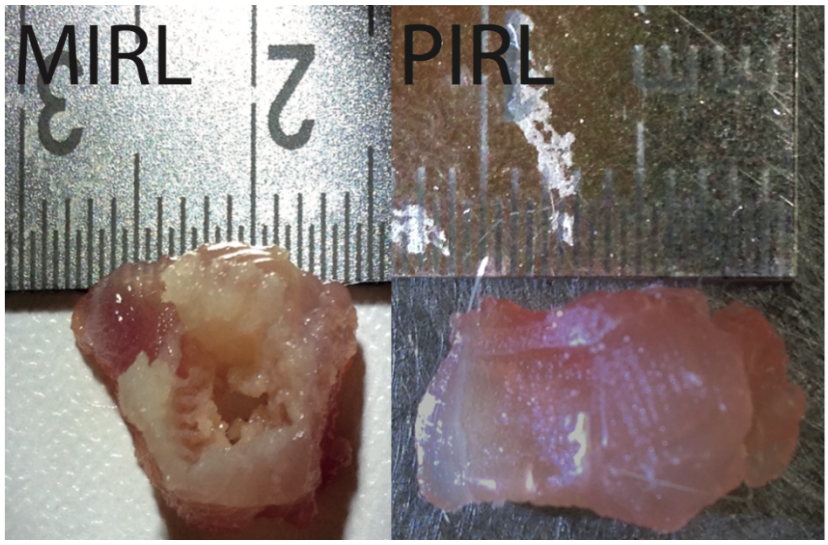

Figure S-4. Ablated rat muscle tissues after 260 seconds of ablation with MIRL (left) and PIRL (right). A 4 x 4 mm area was irradiated in both cases. Burning residue is observed after MIRL irradiation but not for PIRL. For MIRL it is also observed that heat dissipates into adjacent tissue causing collateral heat damage.

6. Ablated rat liver tissues after ablation with PIRL (A) and MIRL (B).

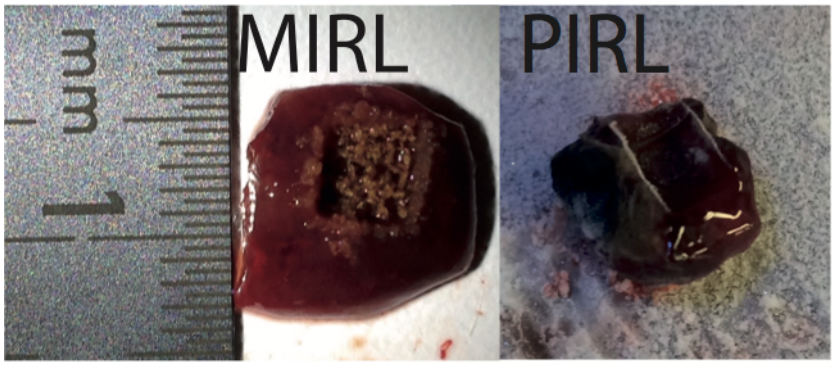

Figure S-5. Ablated rat liver tissues after 260 seconds of ablation with MIRL (left) and PIRL (right). A 4 x 4 mm area was irradiated in both cases. Burning residue is observed after MIRL irradiation but not for PIRL. For MIRL it is also observed that heat dissipates into adjacent tissue causing collateral heat damage.

7. BCA Assay for determine the protein concentration of MIRL and PIRL rat kidney homogenates prior MALDI analysis.

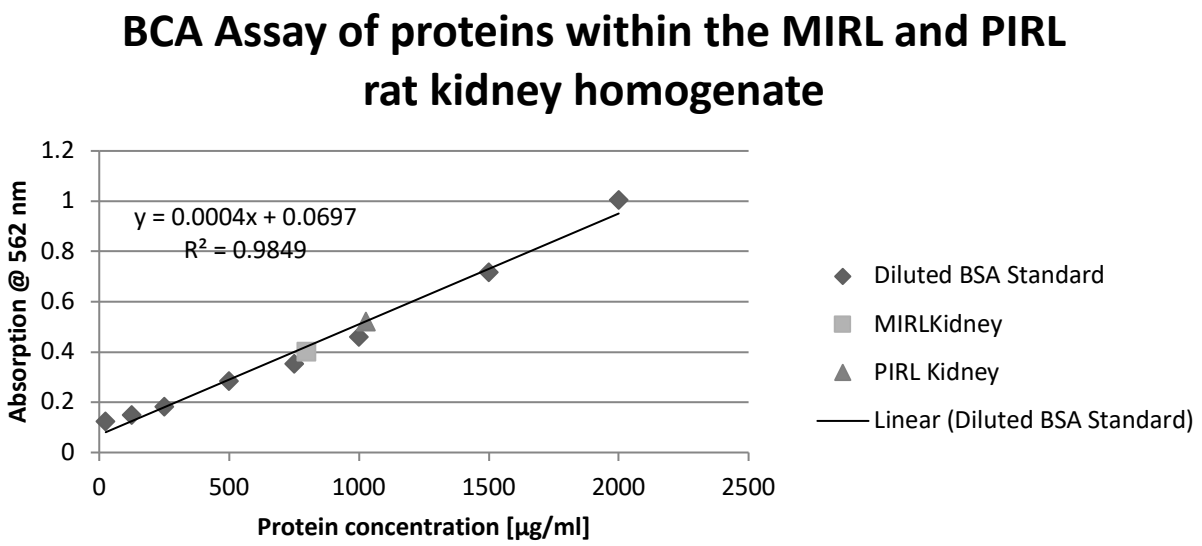

Figure S-6. BCA Assay for determine the protein concentration of MIRL and PIRL rat kidney homogenates prior MALDI analysis. The protein concentration for MIRL homogenate was 801 µg/ml and for PIRL homogenate 1026 µg/ml.